Facial Selectivity of the (*R*)-1,3-Dimethyl-1-Cyclohexyl Cation in the Gas Phase

Antonello Filippi*[a]

Abstract: The model reaction between the (*R*)-1,3-dimethyl-1-cyclohexyl cation (**I**) and methanol has been investigated under gas-phase radiolytic conditions (750 Torr; 25–120 °C) with the aim of evaluating the intrinsic factors that govern the facial selectivity of biased carbocations. The peculiarity of the experimental approach allows the formation of different $CH_3{}^{18}OH \cdot \mathbf{I}$ ionic adducts. Subsequent conversion of these adducts to give the corresponding *E*/*Z* covalent products follows different reaction coordinates, which are characterized by their own activation parameters. On the grounds of density functional theory (DFT) results, several $[CH_3OH \cdot \mathbf{I}]$ structures have been located on the relevant potential-energy surface (PES). The experimental results point to a gas-phase facial selectivity, which is mainly governed by entropic factors that arise as a result of the occurrence of different noncovalent ion–molecule "facial adducts" (FA). The formation of FAs may also play an important role in both the reaction dynamics and the positional selectivity. The present results cannot be interpreted by any of the models based on solution-phase experiments.

Keywords: diastereoselectivity · facial selectivity · gas-phase reactions · ion–molecule reactions · kinetics · noncovalent interactions

Introduction

The growing use of optically pure chiral compounds in many areas of chemistry and biochemistry has recently sparked an intense effort to understand the facial selectivity of planar carbon centers. Over the years, a number of factors have been proposed as having an influence on the facial selectivity of reactive species towards trigonal carbon centers;[1] these include steric hindrance, conformational and chelation effects, and ion pairing, as well as orbital and electronic interactions. Solvation and temperature effects are also important. Assessing the relative roles of these factors is not easy. Reactions of different 2-methyl-5-X-2-adamantyl cations with a number of nucleophiles in condensed media have been investigated by several research groups.[2] All the studies indicate that the facial selectivity of these rigid cations is due to the differential hyperconjugative stabilization of the competing *syn* and *anti* transition states. Irrespective of its electrostatic or orbital origin, such an intrinsic factor should play a major role in the gas phase, owing to the lack of the mediating effects of the solvent. However, a completely different picture emerges from the gas-phase investigation of 2-methyl-5-X-adamantyl cations ($X = F, Si(CH_3)_3$).[3] In this study, which was performed by means of the radiolytic technique, the gas-phase facial selectivity of the selected ions towards methanol was considered to be the result of entropy rather than enthalpy, and the negative activation entropies obtained could be attributed to the increased rigidity of the relevant transition structures. We used the same gas-phase radiolytic approach to evaluate the kinetics of the addition of methanol to a flexible cation, namely, the (*R*)-1,3-dimethyl-1-cyclohexyl cation (**I**). It is hoped that the results of this model reaction will provide greater insight into the role that intrinsic factors play in determining the facial selectivity of biased and conformationally mobile cyclohexyl cations, a class of reactive intermediates recently investigated both experimentally and theoretically.[4]

Results

Gas-phase protonation of the substrate: The radiolytic technique allowed the gas-phase protonation of **1** to be carried out in two ways. In $CH_4/\mathbf{1}/CH_3{}^{18}OH$ mixtures, γ-radiolysis of the bulk gas CH_4 generates stationary concentrations of $C_nH_5{}^+$ ($n = 1,2$) ions. These strong Brønsted acids are able to protonate **1**[5] (path i in Scheme 1) yielding the chiral (*R*)-1,3-dimethyl-1-cyclohexyl cation (**I**) in the presence of small amounts of nucleophile ($CH_3{}^{18}OH$, $^{18}O = 94\,\%$), an efficient radical scavenger (O_2), and a powerful base

[a] Dr. A. Filippi
Dipartimento di Studi di Chimica e Tecnologia delle Sostanze Biologicamente Attive Università degli Studi di Roma "La Sapienza" P.le A. Moro 5, 00185 Roma (Italy)
Fax: (+39) 06-49-91-36-02
E-mail: antonello.filippi@uniroma1.it

Supporting information for this article is available on the WWW under http://www.chemeurj.org/ or from the author.

DOI: 10.1002/chem.200304859

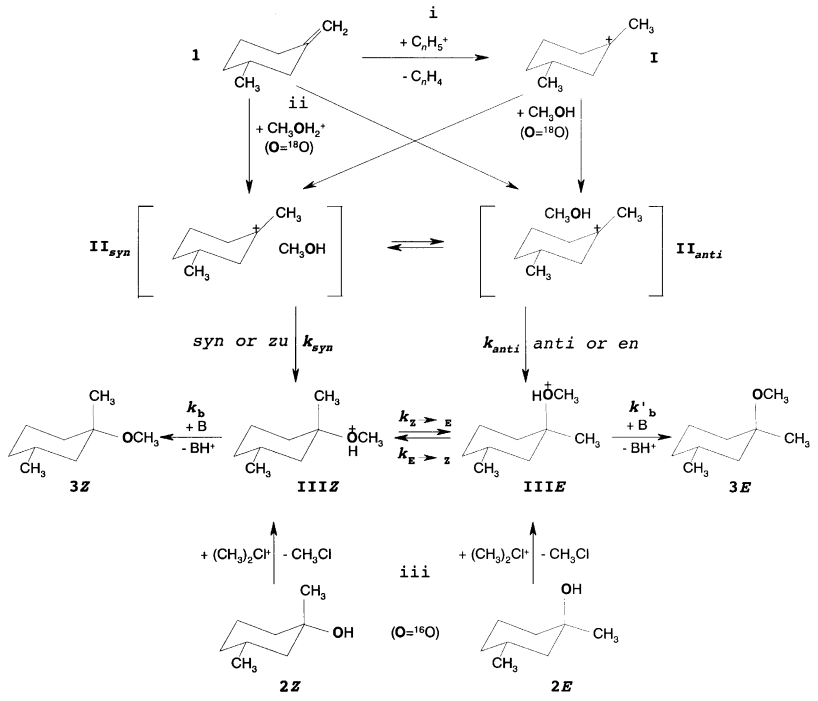

Scheme 1. Reaction pathways for the extracomplex (path i), intracomplex (path ii), and epimerization (path iii) experiments.

Abstract in Italian: *Al fine di valutare il ruolo dei fattori intrinseci che determinano la selettività facciale di carbocationi non simmetrici, la cinetica della reazione fra il metanolo e il catione chirale (R)-1,3-dimetil-1-cicloesile (**I**) è stata studiata in fase gassosa utilizzando la tecnica della radiolisi (750 torr; 25–120 °C). La peculiarità del metodo impiegato consente la formazione di diversi addotti $CH_3{}^{18}OH$–**I**, i quali evolvono verso i corrispondenti prodotti covalenti E/Z seguendo diverse coordinate di reazione, ciascuna caratterizzata da parametri di attivazione specifici. Alcune strutture [$CH_3OH \cdot$ **I**] sono state localizzate mediante uno studio teorico (DFT) della superficie di energia potenziale. I risultati sperimentali evidenziano che, in fase gassosa, la selettività facciale è determinata principalmente da fattori entropici, i quali riflettono la dinamica di reazione di diversi "addotti facciali" ione-molecola non covalenti (FA). La loro formazione può avere un ruolo importante nel determinare sia la dinamica delle reazioni sia la selettività posizionale. I risultati ottenuti non possono essere razionalizzati utilizzando i modelli elaborati sulla base di studi condotti in fase condensata.*

[$(N(C_2H_5)_3)$]. The base ensures that the oxonium-ion intermediates are efficiently deprotonated (k_b and k'_b in Scheme 1). In CH_3F/**1**/$H_2{}^{18}O$ mixtures, γ-radiolysis of CH_3F generates stationary concentrations of $(CH_3)_2F^+$, whose reaction with $H_2{}^{18}O$ yields $CH_3{}^{18}OH_2^+$ ions, in the absence of any neutral $CH_3{}^{18}OH$ molecules.[6] The so formed $CH_3{}^{18}OH_2^+$ then acts both as a Brønsted acid catalyst[7] (path ii in Scheme 1) and as a nucleophile ($CH_3{}^{18}OH$) generator. The substantial difference between the two approaches is that, in route i (henceforth called the extracomplex route), the products (1*R*,3*R*)-1-methoxy-1,3-dimethylcyclohexane (**3*E***) and (1*S*,3*R*)-1-methoxy-1,3-dimethylcyclohexane (**3*Z***) arise when external $CH_3{}^{18}OH$ molecules present in the gaseous mixture react with preformed **I** to firstly give the encounter complexes $\mathbf{II}_{syn}$ and $\mathbf{II}_{anti}$. On the other hand, in route ii (henceforth called the intracomplex route), the same products arise from the intimate $\mathbf{II}_{syn}$ and $\mathbf{II}_{anti}$ complexes characterized by an initial specific orientation between the incipient ion **I** and the incipient $CH_3{}^{18}OH$ molecule, which is internally generated by proton transfer from $CH_3{}^{18}OH_2^+$ to **1**. The high pressure of the inert gaseous medium (CH_4 or CH_3F; 750 Torr) ensures effective collisional thermalization ($7-50\times10^9$ collisions s^{-1})[8] of the ion–molecule complexes before their conversion to **III*Z*** and **III*E*** (vide infra).

To evaluate the extent of oxonium-ion epimerization (**III*E*** $\rightleftharpoons$ **III*Z***, $k_{E\rightarrow Z}$ and $k_{Z\rightarrow E}$ in Scheme 1) prior to neutralization, a third set of experiments was performed with (1*R*,3*R*)-1,3-dimethylcyclohexanol (**2*E***) or (1*S*,3*R*)-1,3-dimethylcyclohexanol (**2*Z***) (enantiomeric excess (*ee*) ca. 99%) as the starting substrates, CH_3Cl as the bulk gas, and traces of $H_2{}^{18}O$, O_2, and $N(C_2H_5)_3$. γ-Irradiation of such gaseous mixtures generates stationary concentrations of the Lewis acid $(CH_3)_2Cl^+$, which barely reacts with $H_2{}^{18}O$,[9] but which is strong enough to methylate the alcoholic chiral substrates to yield the corresponding oxonium intermediates **III*E*** and **III*Z*** (path iii in Scheme 1).[10] All the irradiations were performed at a constant temperature in the range 25–120 °C.

Radiolytic experiments: The upper part of Table 1 reports the relative distribution and the total absolute yield of the ^{18}O-labeled ethereal products (**3*E*** and **3*Z***) obtained from the γ-irradiated CH_4/**1**/$CH_3{}^{18}OH$ gaseous mixtures (the extracomplex reaction). The product yields from the CH_3F/**1**/$H_2{}^{18}O$ mixtures (the intracomplex reaction) are reported in the lower part of Table 1. Over 95% of the ^{18}O incorporated into **3*E*** and **3*Z*** occurs through the extracomplex reaction; this is in agreement with the isotopic composition of the nucleophile ($CH_3{}^{18}OH$, $^{18}O = 94\%$). For the same products in the intracomplex reaction (CH_3F/**1**/$H_2{}^{18}O$ systems), this percentage decreases to 50%, due to the presence of ubiquitous $H_2{}^{16}O$[11] in the gaseous mixtures. However, the yield of both labeled or unlabeled **3*E*** and **3*Z*** decreases substantially (by over 80%) when the molar fraction of the strong base $N(C_2H_5)_3$ is quintupled in the starting mixtures; this is evidence that the ethereal products in Table 1 are ionic in origin.

Table 1. Relative distribution of the ^{18}O-labeled ethereal products from attack of methanol on **I** in the gas phase.[a]

	T [°C]	$CH_3{}^{18}OH$ [Torr]	B [Torr]	τ[c] [$\times 10^8$ s]	**3*E***[d]	**3*Z***[d]	$G_{(M)}$[e]
path i[b]							
	25	1.05	0.70	3.61	0.463	0.537	0.99
	40	1.06	0.67	4.01	0.485	0.515	0.92
	40	1.17	0.69	3.88	0.473	0.527	0.67
	40	0.53	0.59	4.49	0.482	0.518	0.52
	50	0.92	0.71	3.89	0.510	0.490	0.60
	60	1.04	0.71	4.02	0.502	0.498	0.53
	60	0.97	0.71	4.02	0.477	0.523	0.84
	70	1.14	0.75	3.94	0.510	0.490	0.48
	80	1.03	0.69	4.41	0.509	0.491	0.59
	80	1.03	0.70	4.36	0.487	0.513	0.37
	100	0.56	0.79	3.34	0.511	0.489	0.43
	100	1.12	0.75	4.28	0.498	0.502	0.83
path ii[f]							
	25	3.10	0.70	3.61	0.450	0.550	0.06
	40	2.89	0.71	3.76	0.436	0.564	0.11
	50	3.02	0.72	3.81	0.424	0.576	0.12
	50	3.02	0.73	3.77	0.419	0.581	0.14
	60	3.12	0.71	4.02	0.420	0.580	0.13
	70	3.01	0.68	4.31	0.400	0.600	0.07
	70	3.13	0.68	4.32	0.402	0.598	0.10
	80	2.90	0.65	4.69	0.412	0.588	0.11
	100	2.97	0.73	4.43	0.409	0.591	0.08

[a] Substrate **1** (0.5 Torr), O_2 (5 Torr), $B = N(C_2H_5)_3$; radiation dose 1×10^4 Gy (dose rate $= 5 \times 10^3$ Gy h^{-1}). [b] The extracomplex pathway; bulk gas CH_4 (750 Torr). [c] Reaction time, calculated as the reciprocal of the pseudo-first-order collision constant between intermediates **III*E*** and **III*Z*** and B (ref. [8]). [d] Mean values from repeated experiments; uncertainty level ca. 5%. [e] $G_{(M)}$ = number of molecules M produced per 100 eV of absorbed energy. [f] The intracomplex pathway; bulk gas CH_3F (750 Torr).

In the CH_4/**1**/$CH_3{}^{18}OH$ experiments, besides the ethereal products, appreciable amounts of unlabeled **2*E*** and **2*Z***, as well as (*R*)-1,3-dimethylcyclohexene and (*R*)-1,5-dimethylcyclohexene are formed. In the CH_3F/**1**/$H_2{}^{18}O$ mixtures, the ethereal products are accompanied by ^{18}O-labeled **2*E*** and **2*Z*** in yields that are comparable to those obtained for the unlabeled analogues. The alcoholic products **2*E*** and **2*Z*** are thought to arise from attack of the free **I** ion by labeled and/or unlabeled[11] water molecules followed by $N(C_2H_5)_3$-neutralization of the oxonium intermediates so formed. Direct $N(C_2H_5)_3$-deprotonation of **I** is the most probable route to the formation of (*R*)-1,3-dimethylcyclohexene and (*R*)-1,5-dimethylcyclohexene. The fact that the diastereomeric ^{18}O-labeled products are not accompanied by their enantiomers indicates that the tertiary cation **I** does not undergo extensive prototropic rearrangement. Therefore, the neutral ^{18}O-labeled products **3*E*** and **3*Z*** do indeed arise from the reactions depicted in Scheme 1. If the efficiency of the deprotonation steps (k_b and k'_b) depicted in Scheme 1 are taken to be equal, the relative quantities of neutral ^{18}O-labeled products **3*E*** and **3*Z*** reflect those of the corresponding oxonium intermediates **III*E*** and **III*Z***.[12] The k_{syn}/k_{anti} ratio can then be inferred from the relative concentration of **III*E*** and **III*Z***, once the extent of their interconversion, under the same experimental conditions, is considered. To this end, intermediates **III*E*** and **III*Z*** were generated by path iii in Scheme 1, and their epimerization constants ($k_{E\rightarrow Z}$ and $k_{Z\rightarrow E}$) were calculated using the Equations (1a) – (1d):[3]

$$k_{Z\rightarrow E} = \frac{\varepsilon_{eq}}{\tau}\ln\left\{\frac{\varepsilon_{eq}}{\varepsilon_{eq}-\varepsilon}\right\} \quad (1a)$$

$$\varepsilon_{eq} = \frac{K_{eq}}{1+K_{eq}} \quad (1b)$$

$$k_{E\rightarrow Z} = \frac{\zeta_{eq}}{\tau}\ln\left\{\frac{\zeta_{eq}}{\zeta_{eq}-\zeta}\right\} \quad (1c)$$

$$\zeta_{eq} = \frac{1}{1+K_{eq}} \quad (1d)$$

whereby ε and ζ indicate the extent of epimerization of **III*Z*** and **III*E***, respectively, during their lifetime τ. These epimerization factors are evaluated as the molar fraction of unlabeled ethers, **3*E*** and **3*Z***, obtained from the chiral alcohols **2*Z*** and **2*E***, respectively.

At any given temperature, the **III*Z*** $\rightleftharpoons$ **III*E*** equilibrium constant (K_{eq}) can be calculated from Equation (2). The results are given in Table 2.

$$K_{eq} = \frac{\varepsilon}{\zeta} \quad (2)$$

Table 2. Kinetics of the gas-phase epimerization of **III*E*** and **III*Z***.[a]

Substrate	T [°C]	B [Torr]	τ[b] [$\times 10^8$ s]	ζ[c]	$k_{E\rightarrow Z}$[d] [$\times 10^{-6}$ s^{-1}]	K_{eq}[d]
2*E*	25	0.74	3.40	0.047	1.44 (6.16)	0.58 (−0.24)
2*E*	40	0.71	3.75	0.060	1.68 (6.23)	0.62 (−0.21)
2*E*	50	0.71	3.88	0.106	3.01 (6.48)	0.67 (−0.17)
2*E*	60	0.69	4.14	0.135	3.69 (6.57)	0.67 (−0.17)
2*E*	70	0.71	4.11	0.168	4.87 (6.69)	0.80 (−0.09)
2*E*	80	0.66	4.57	0.238	6.81 (6.83)	0.80 (−0.10)
2*E*	100	0.64	5.00	0.281	8.23 (6.92)	0.99 (0.00)
2*E*	120	0.63	5.38	0.464	17.07 (7.23)	0.70 (−0.15)
Substrate	T [°C]	B [Torr]	τ[b] [$\times 10^8$ s]	ε[c]	$k_{Z\rightarrow E}$[d] [$\times 10^{-6}$ s^{-1}]	K_{eq}[d]
2*Z*	25	0.75	3.37	0.027	0.83 (5.92)	0.58 (−0.24)
2*Z*	40	0.74	3.61	0.037	1.08 (6.03)	0.62 (−0.21)
2*Z*	50	0.71	3.88	0.071	2.01 (6.30)	0.67 (−0.17)
2*Z*	60	0.67	4.24	0.091	2.43 (6.39)	0.67 (−0.17)
2*Z*	70	0.71	4.11	0.135	3.92 (6.59)	0.80 (−0.09)
2*Z*	80	0.67	4.51	0.191	5.53 (6.74)	0.80 (−0.10)
2*Z*	100	0.65	4.94	0.279	8.29 (6.92)	0.99 (0.00)
2*Z*	120	0.65	5.23	0.327	12.37 (7.09)	0.70 (−0.15)

[a] Substrate (0.5 Torr), bulk gas CH_3Cl (750 Torr), O_2 (5 Torr), $H_2{}^{18}O$ (ca. 3 Torr), $B = N(C_2H_5)_3$; radiation dose 1×10^4 Gy (dose rate $= 5 \times 10^3$ Gy h^{-1}). [b] Reaction time, calculated as the reciprocal of the pseudo-first-order collision constant between intermediates **III*E*** and **III*Z*** and B (ref. [8]). [c] $\zeta = [\mathbf{3}\boldsymbol{E}]/([\mathbf{3}\boldsymbol{E}]+[\mathbf{3}\boldsymbol{Z}])$ and $\varepsilon = [\mathbf{3}\boldsymbol{E}]/([\mathbf{3}\boldsymbol{E}]+[\mathbf{3}\boldsymbol{Z}])$ are mean values from repeated experiments; uncertainty level ca. 5%; ^{18}O-ethers < 3%. [d] See text for k and K_{eq} definitions; $\log k$ and $\log K_{eq}$ in parentheses.

Linear correlations were found between $\log k_{E\rightarrow Z}$ (and $\log k_{Z\rightarrow E}$) and T^{-1}. A similar correlation was also obtained for $\log K_{eq}$ ($\log K_{eq} = (0.5 \pm 0.3) - (0.9 \pm 0.4)1000/(2.303\,RT)$; $r^2 = 0.533$), as depicted in Figure 1.

Table 3 gives the relevant Arrhenius equations and the corresponding activation parameters calculated according to the transition-state theory. Activation enthalpies indicate that **III*Z*** is more stable than **III*E*** by 0.9 kcal mol^{-1}.

The Arrhenius equations in Table 3 allow the ε and ζ terms for each τ value in Table 1 to be evaluated. In turn, this data,

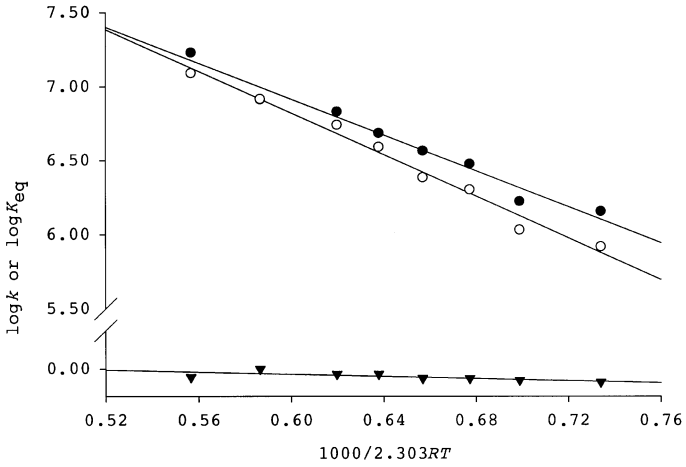

Figure 1. Temperature dependence of $\log k_{E\rightarrow Z}$ (full circles), $\log k_{Z\rightarrow E}$ (open circles), and $\log K_{eq}$ (full triangles) for the epimerization reaction **III*E*** $\rightleftharpoons$ **III*Z***.

Table 3. Kinetics of the epimerization of **III*Z*** and **III*E*** in the gas phase: Arrhenius equations and relevant activation parameters.

Arrhenius equation[a]	corr. Coeff r^2	$\Delta H^{\neq}$ [kcal mol^{-1}]	$\Delta S^{\neq}$ [cal mol^{-1} K^{-1}]
$\log k_{E\rightarrow Z} = (10.6 \pm 0.3) - (6.1 \pm 0.4)x$	0.974	5.5 ± 0.4	-12.1 ± 1.2
$\log k_{Z\rightarrow E} = (11.0 \pm 0.2) - (7.0 \pm 0.4)x$	0.985	6.4 ± 0.4	-9.9 ± 1.1

[a] $x = 1000/2.303\,RT$.

along with the molar concentrations of **3*E*** and **3*Z*** given in Table 2, have been used to calculate the k_{syn}/k_{anti} ratio by using Equation (3).[3]

$$\frac{k_{syn}}{k_{anti}} = \frac{[\mathbf{3}Z] - \zeta}{[\mathbf{3}E] - \varepsilon} \qquad (3)$$

The results for both the extracomplex and intracomplex reactions are plotted as $\log(k_{syn}/k_{anti})$ against T^{-1} in Figure 2.

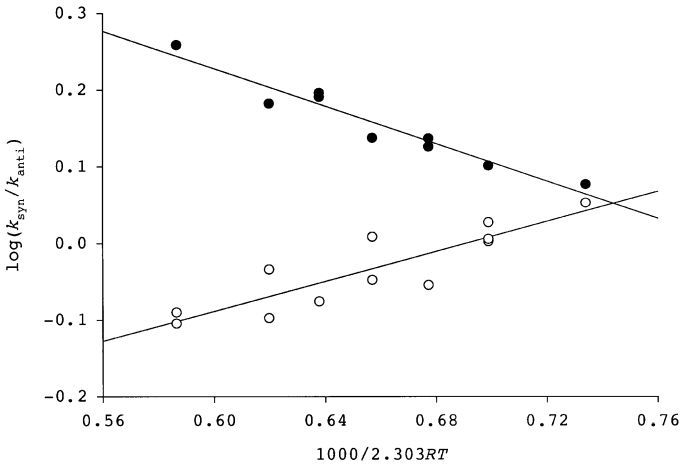

Figure 2. Differential Arrhenius plots ($\log(k_{syn}/k_{anti})$ vs T^{-1}) for intracomplex (full circles) and extracomplex (open circles) attack of ion **I** by methanol in the gas phase.

The relevant differential Arrhenius equations and the corresponding activation parameters were calculated from the slope and *y* axis intercept of the straight lines obtained by linear regression analysis (Table 4). Surprisingly, opposite differential activation parameters are observed. The entropic contributions are large enough to invert the enthalpic facial selectivity in both the extra- ($T > 43\,^{\circ}$C) and the intracomplex ($T > 5\,^{\circ}$C) reaction.

Table 4. Differential Arrhenius equations and relevant differential activation parameters for extracomplex (i) and intracomplex (ii) attack of methanol on **I** in the gas phase.

Path	Arrhenius equation[a]	corr. coeff. r^2	$\Delta\Delta H^{\neq}$ [kcal mol^{-1}]	$\Delta\Delta S^{\neq}$ [cal mol^{-1} K^{-1}]
i	$\log(k_{syn}/k_{anti}) = (-0.7 \pm 0.1) - (-1.0 \pm 0.2)x$	0.773	-1.0 ± 0.2	-3.1 ± 0.5
ii	$\log(k_{syn}/k_{anti}) = (1.0 \pm 0.1) - (1.2 \pm 0.1)x$	0.933	1.2 ± 0.1	4.4 ± 0.4

[a] $x = 1000/2.303\,RT$.

Theoretical calculations: A comprehensive and high-level ab initio investigation of the PES of the reaction network depicted in Scheme 1 is practically inaccessible either intrinsically, because of the conformational mobility of the system, and computationally, because of the need for an extended basis set. However, several critical points have been located at the B3LYP/6 – 31G* level of theory;[13] their energies are reported in Table 5, while the relevant optimized structures are shown in Figure 3. It is worth noting that the structural

Table 5. B3LYP/6-31G*//B3LYP/6-31G* results.

	E[a] [Hartree]	ZPE[b] [Hartree]	E + ZPE [Hartree]	E + ZPE [kcal mol^{-1}]
CH_3OH	– 115.714406	0.051458	– 115.662948	
$CH_3OH_2^+$	– 116.015745	0.064381	– 115.951364	
$\mathbf{1}_{eq}$[c]	– 313.278724	0.203706	– 313.075018	0.0
$\mathbf{1}_{ax}$	– 313.276204	0.203943	– 313.072261	1.7
$\mathbf{I}_{eq}$	– 313.620403	0.214103	– 313.406300	0.0
$\mathbf{I}_{ax}$	– 313.616850	0.214188	– 313.402662	2.3
III E	– 429.364812	0.271732	– 429.093080	0.0
III Z	– 429.364040	0.271748	– 429.092292	0.5
$\mathbf{II}_{anti}$	– 429.353500	0.267317	– 429.086183	4.3
$\mathbf{II a}_{syn}$	– 429.353348	0.267151	– 429.086197	4.3
$\mathbf{II b}_{syn}$	– 429.352705	0.267255	– 429.085450	4.8
$\mathbf{TS}_{inv}$[d]	– 429.350565	0.266908	– 429.083657	5.9
$\mathbf{I}_{eq} + CH_3OH$	– 429.334810	0.265561	– 429.069249	15.0
$\mathbf{1}_{eq} + MeOH_2^+$	– 429.294469	0.268087	– 429.026382	41.8

[a] Total energy. [b] Zero-point energy. [c] Calculated B3LYP/6-31G* proton affinity: 208.9 kcal mol^{-1}. [d] Imaginary frequency: i64.92 cm^{-1}.

deformation of both $\mathbf{I}_{eq}$ and $\mathbf{I}_{ax}$ is similar to that of the C–C hyperconjomer of the 1-methylcyclohexyl cation.[4a] In particular, there is: 1) bond elongation of C2–C3 and C5–C6; 2) C–H bond elongation in the methyl group, which eclipses the empty p orbital; 3) C1–C2–C3 angle contraction; and 4) slight equatorial pyramidalization ($\mathbf{I}_{eq} = 172.39^{\circ}$; $\mathbf{I}_{ax} = 173.37^{\circ}$) of the charged C1 atom. Also, at least at the B3LYP/6 – 31G* level of theory, a C–H hyperconjomer of **I** (the carbocation

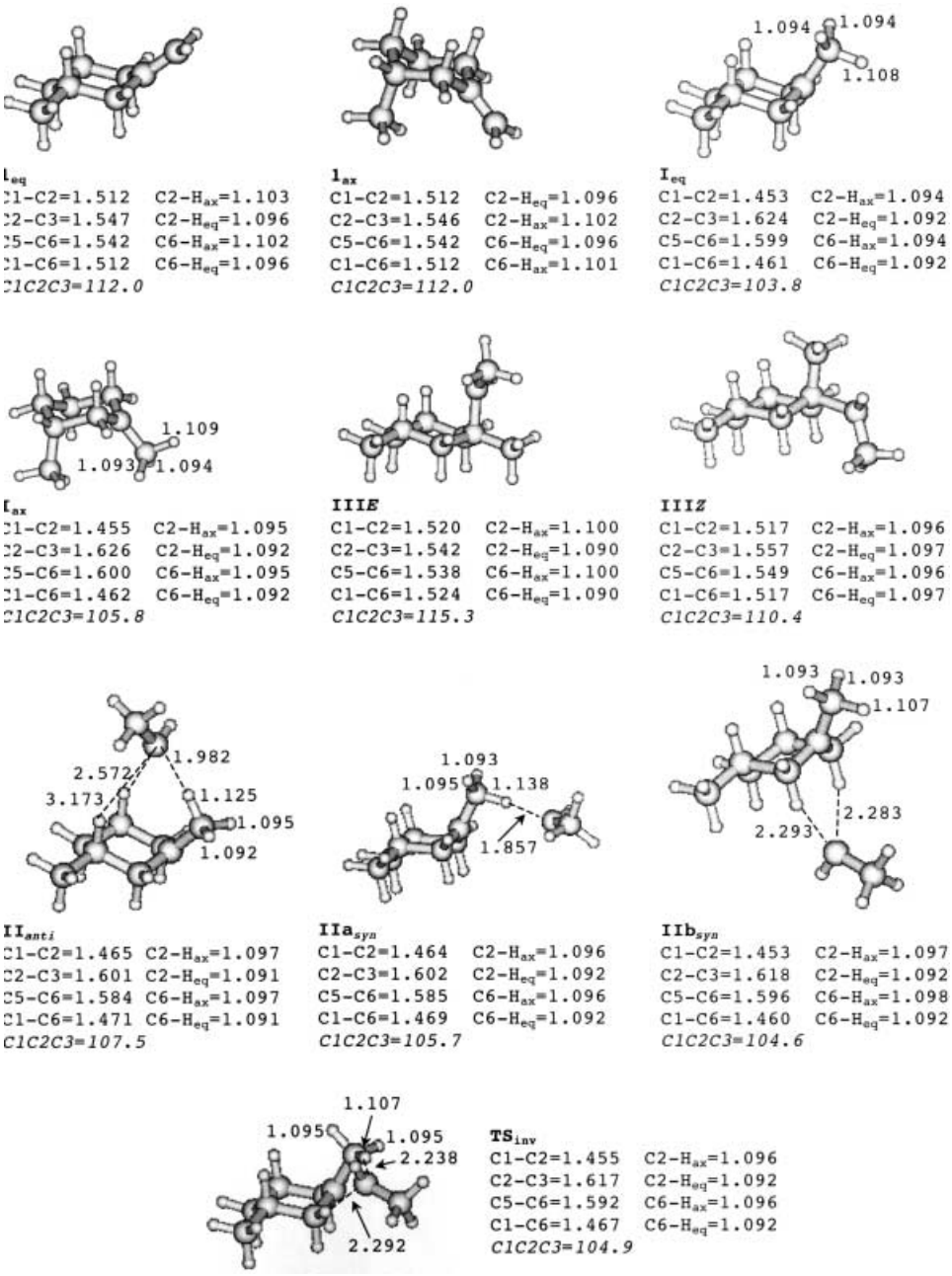

$\mathbf{1}_{eq}$
C1-C2=1.512 C2-H_{ax}=1.103
C2-C3=1.547 C2-H_{eq}=1.096
C5-C6=1.542 C6-H_{ax}=1.102
C1-C6=1.512 C6-H_{eq}=1.096
C1C2C3=112.0

$\mathbf{1}_{ax}$
C1-C2=1.512 C2-H_{eq}=1.096
C2-C3=1.546 C2-H_{ax}=1.102
C5-C6=1.542 C6-H_{eq}=1.096
C1-C6=1.512 C6-H_{ax}=1.101
C1C2C3=112.0

$\mathbf{I}_{eq}$
C1-C2=1.453 C2-H_{ax}=1.094
C2-C3=1.624 C2-H_{eq}=1.092
C5-C6=1.599 C6-H_{ax}=1.094
C1-C6=1.461 C6-H_{eq}=1.092
C1C2C3=103.8

$\mathbf{I}_{ax}$
C1-C2=1.455 C2-H_{ax}=1.095
C2-C3=1.626 C2-H_{eq}=1.092
C5-C6=1.600 C6-H_{ax}=1.095
C1-C6=1.462 C6-H_{eq}=1.092
C1C2C3=105.8

III*E*
C1-C2=1.520 C2-H_{ax}=1.100
C2-C3=1.542 C2-H_{eq}=1.090
C5-C6=1.538 C6-H_{ax}=1.100
C1-C6=1.524 C6-H_{eq}=1.090
C1C2C3=115.3

III*Z*
C1-C2=1.517 C2-H_{ax}=1.096
C2-C3=1.557 C2-H_{eq}=1.097
C5-C6=1.549 C6-H_{ax}=1.096
C1-C6=1.517 C6-H_{eq}=1.097
C1C2C3=110.4

$\mathbf{II}_{anti}$
C1-C2=1.465 C2-H_{ax}=1.097
C2-C3=1.601 C2-H_{eq}=1.091
C5-C6=1.584 C6-H_{ax}=1.097
C1-C6=1.471 C6-H_{eq}=1.091
C1C2C3=107.5

$\mathbf{IIa}_{syn}$
C1-C2=1.464 C2-H_{ax}=1.096
C2-C3=1.602 C2-H_{eq}=1.092
C5-C6=1.585 C6-H_{ax}=1.096
C1-C6=1.469 C6-H_{eq}=1.092
C1C2C3=105.7

$\mathbf{IIb}_{syn}$
C1-C2=1.453 C2-H_{ax}=1.097
C2-C3=1.618 C2-H_{eq}=1.092
C5-C6=1.596 C6-H_{ax}=1.098
C1-C6=1.460 C6-H_{eq}=1.092
C1C2C3=104.6

$\mathbf{TS}_{inv}$
C1-C2=1.455 C2-H_{ax}=1.096
C2-C3=1.617 C2-H_{eq}=1.092
C5-C6=1.592 C6-H_{ax}=1.096
C1-C6=1.467 C6-H_{eq}=1.092
C1C2C3=104.9

Figure 3. Optimized structures and relevant geometrical parameters of the critical points located on the [$CH_3OH \cdot \mathbf{I}$] PES at the B3LYP/6–31G* level of theory. Bond lengths are given in Å, angles are italicized and given in degrees.

axially oriented by C2–H_{ax} and C6–H_{ax} hyperconjugation) does not exist. This could be due to the fact that **I** contains just one 3-methyl group.[4b]

According to the $E+ZPE$ column of Table 5, the $\mathbf{1}_{eq}$ and $\mathbf{I}_{eq}$ chair structures, in which the methyl group is equatorial, are 1.7 and 2.3 kcal mol^{-1} more stable than the corresponding chair conformers, $\mathbf{1}_{ax}$ and $\mathbf{I}_{ax}$, respectively. This is in agreement with the experimental value obtained for the conformational energy of the methyl group (1.9–2.1 kcal mol^{-1}).[4b, 14] Therefore, $\mathbf{1}_{eq}$ and $\mathbf{I}_{eq}$ are, by far, the most abundant conformers of **1** and **I**. The oxonium ion **III*E*** has the lowest $E+ZPE$ value on the [$\mathbf{I} \cdot CH_3OH$] PES (C1–O binding energy: 15.0 kcal mol^{-1}), while diastereomer **III*Z*** is 0.5 kcal mol^{-1} higher in energy. Epimerization of the two species involves the transition structure $\mathbf{TS}_{inv}$ (5.9 kcal mol^{-1} higher than **III*E***). Taking into account the uncertainty of the method used (ca. 2 kcal mol^{-1}),[15] the theoretical results correspond closely to those obtained experimentally (Table 3: $\Delta H^{\neq}_{Z\rightarrow E} =$ 6.4 kcal mol^{-1}; ΔH°(**III*Z*** $\rightleftharpoons$ **III*E***) = 0.9 kcal mol^{-1}). Only a single $\mathbf{II}_{anti}$ structure (4.3 kcal mol^{-1}) has been located, but two different *syn* adducts have been found; $\mathbf{IIa}_{syn}$ (4.3 kcal mol^{-1}), which has a single methyl C–H interaction, and the less stable $\mathbf{IIb}_{syn}$ (4.8 kcal mol^{-1}), in which the oxygen atom is coordinated to both the axial C2 and C6 hydrogen atoms. At the same level of theory, the proton affinity of 3-methyl-1-methylenecyclohexane (208.9 kcal mol^{-1}) has also been calculated.

Discussion

The addition reaction: In the intracomplex reaction, enthalpy favors *anti* rather than *syn* attack of **I** by methanol (1.2 kcal mol^{-1}) (Table 4). However, as a result of entropy (4.4 cal mol^{-1} K^{-1}), at $T > 5\,^{\circ}C$ *syn* attack predominates. A completely different result arises in the extracomplex experiments: although enthalpy (−1.0 kcal mol^{-1}) favours *syn* attack, entropy (−3.1 cal mol^{-1} K^{-1}) reverses the selectivity at $T > 43\,^{\circ}C$. Such divergent results obtained for the same reaction (Figure 2) cannot be interpreted in terms of any of the theories so far proposed to explain the facial selectivity of trigonal carbon centers,[1, 16, 17] but must be related to the different behavior of the reactive intermediates in the extra- and intracomplex reactions.

As reported in the previous section, the vastly different proton affinities of the involved species ensures that ion–molecule adducts like $\mathbf{II}_{syn}$ and $\mathbf{II}_{anti}$ (Scheme 1) are stable intermediates in both the extra- and intracomplex reaction. The hypothesis that $\mathbf{II}_{syn}$ and $\mathbf{II}_{anti}$ reach a rapid equilibrium prior to being converted into **III*Z*** and **III*E*** is not supported

by the present results. In fact, the plots in Figure 2 clearly indicate that in the extra- and intracomplex attack of **I** by methanol, facial selectivity has a different temperature dependence, which is the result of opposite $\Delta\Delta H^{\neq}$ and $\Delta\Delta S^{\neq}$ contributions to $\Delta\Delta G^{\neq}$. The alternative hypothesis that the $\mathbf{II}_{syn}$ and $\mathbf{II}_{anti}$ intermediates react through the same species in both the extra- and intracomplex reaction is also not supported by the current results. In fact, because different reaction partners are involved (steps i and ii in Scheme 1), it is likely that the relative populations of $\mathbf{II}_{syn}$ and $\mathbf{II}_{anti}$ formed are not the same, contributing to the difference in $\Delta\Delta S^{\neq}$ values seen in Table 4. Moreover, the presence of the same $\mathbf{II}_{syn}$ and $\mathbf{II}_{anti}$ reactive structures in the two processes should lead to the same $\Delta\Delta H^{\neq}$ values, in contrast to the experimental evidence. From this analysis, the experimental results clearly indicate that: 1) along the extra- and intracomplex reaction pathways, the $\mathbf{II}_{syn}$ and/or $\mathbf{II}_{anti}$ structures are different and their relative abundance depends on the formation process (i or ii in Scheme 1); and 2) interconversion among different $\mathbf{II}_{syn}$ structures must be slow relative to their conversion into **III*Z***. The same holds true for the $\mathbf{II}_{anti}$ adducts.

The occurrence of different "facial adducts" (FAs) between methanol and **I**, that is, noncovalent ion – molecule adducts in which the neutral molecule is coordinated to different points on the same face of the ion, is not unexpected. Indeed, proton transfer from $CH_3{}^{18}OH_2{}^+$ to **1** (path ii in Scheme 1) is thought to lead to the **II a**$_{syn}$ and $\mathbf{II}_{anti}$ adducts depicted in Figure 3, in which the $CH_3{}^{18}OH$ molecule is primarily coordinated to a methyl hydrogen atom of $\mathbf{I}_{eq}$. In contrast, more than one center of interaction on both faces of **I** is kinetically accessible to $CH_3{}^{18}OH$ (path i in Scheme 1). The theoretical results (Table 5 and Figure 3) support the above view, and suggest that a single adduct (**II a**$_{syn}$) is generated in the *syn* intracomplex reaction, while two different FAs (**II a**$_{syn}$ and **II b**$_{syn}$) are involved in the *syn* extracomplex process. On the other hand, the $\mathbf{II}_{anti}$ adduct is favored in both extra- and intracomplex *anti* attack.

Facial selectivity: Conversion of **II** to the corresponding oxonium ions **III*E*** and **III*Z*** must involve rather small activation barriers. This point is supported by: 1) the relatively low experimental activation enthalpy for **III*E*** $\rightleftharpoons$ **III*Z*** epimerization (6.4 kcal mol^{-1}), 2) the poor dependence of the absolute yields of the ethereal products **3*E*** and **3*Z*** upon temperature ($G_{(M)}$ in Table 1), and 3) the computational evidence. Moreover, since the theoretical results indicate that an identical $\mathbf{II}_{anti}$ adduct is involved in the *anti* attack of **I** by methanol in both the extra- and intracomplex reaction, the $\Delta\Delta H^{\neq}$ values in Table 4 suggest that $\Delta H^{\neq}$ for the *syn* extracomplex reaction (**II b**$_{syn}$ $\rightarrow$ **III*Z***) is approximately 2.2 kcal mol^{-1} lower in energy than $\Delta H^{\neq}$ for the *syn* intracomplex reaction (**II a**$_{syn}$ $\rightarrow$ **III*Z***). It should be noted, that this value is 4.4 times greater than the theoretical **II b**$_{syn}$ – **II a**$_{syn}$ relative energy (Table 5: 4.8 – 4.3 = 0.5 kcal mol^{-1}); this suggests that the *syn* transition-state structures involved in the conversion of **II b**$_{syn}$ and **II a**$_{syn}$ to **III*Z*** are different.

The occurrence of more than one FA has already been reported by Speranza et al. in their paper on the isomerization of protonated *para-sec*-butyltoluenes in the gas phase.[18] If one considers, in the absence of solvent-mediating properties, that any type of interaction is better than none, the existence of FAs in gas-phase ion-neutral reactions should be rather common. In fact, when an ion and a neutral molecule approach each other, more than one reciprocal stabilizing interaction can be sought. FAs that interconvert quickly will not be kinetically distinguishable, but if their conversion to the corresponding σ-bonded intermediates is faster than their interconversion, they will dictate the reaction troposelectivity.[19] Indeed, in the latter case, the relative populations of different FAs that operate along parallel reaction coordinates will reflect the positional selectivity.[18] However, if converging reaction coordinates are involved, these will contribute to the overall kinetic constant (as in the *syn* extracomplex reaction: **II a**$_{syn}$ $\rightarrow$ **III*Z*** $\leftarrow$ **II b**$_{syn}$).

As similar investigations in solution have not been conducted, a direct comparison of the present gas-phase results cannot be made. Facial selectivity observed in condensed media has often been interpreted on the grounds of intrinsic stereoelectronic factors, which favor *anti* attack by nucleophilic reagents of both charged and neutral unsaturated carbon atoms of methylenecyclohexane derivatives and their carbonyl analogues.[1, 16, 17] This enthalpic approach assumes that entropic factors in the competing *syn* and *anti* processes are compensating or negligible, which can be accepted only in low-temperate investigations. The present investigation, along with a previous report in which the rigid 2-methyl-5-X-2-adamantyl cation (X = F, $Si(CH_3)_3$) was used, suggests that facial selectivity of charged trigonal carbon centers in the gas phase is strongly influenced by entropic rather than enthalpic factors. A comprehensive analysis of the geometric parameters for the structures in Figure 3 indicates that hyperconjugation may play a role, but, above all, it suggests that facial selectivity in the gas phase is strongly dependent upon the intrinsic ability of both the ionic substrate and the nucleophile to make different ion – molecule adducts, and on their evolution dynamics. In the condensed phase, the solvent cage not only modifies the intrinsic hyperconjugative features of ions like **I**,[4b] but it also mediates the electrostatic interaction between the ion and the neutral nucleophile. Thus, the pronounced solvent effect on the facial selectivity of biased substrates in the condensed phase[1] may be primarily ascribed to the polarizability and dielectric properties of the solvent, and to differential face solvation.[4b]

Conclusion

The kinetics of the reaction between methanol and the (*R*)-1,3-dimethyl-1-cyclohexyl cation (**I**) have been investigated in the gas phase using the radiolytic technique at a pressure of 750 Torr and temperatures ranging from 25 to 120 °C. The results have revealed that entropy contributes to the free activation energy of the competing *syn* and *anti* processes, and plays a major role in determining the facial selectivity by increasing the temperature. The key role of a number of FAs, as suggested by experimental differential activation parameters, is further supported by DFT calculations. The combined results indicate that gas-phase facial selectivity of biased

carbocations is mainly dependent upon the intrinsic aptitude of both the ionic substrate and the neutral nucleophile to form different FAs, and upon the reaction dynamics whereby these FAs interconvert or form the products. FAs are common intermediates in gas-phase ion chemistry, while their occurrence in condensed media may be mediated by solvation.

Experimental Section

Materials: Methane, methyl fluoride, methyl chloride, and oxygen were high-purity gases, which were purchased from UCAR Specialty Gases N.V., and used without further purification. $H_2{}^{18}O$ ($^{18}O = 94.6\,\%$) and $CH_3{}^{18}OH$ ($^{18}O = 94\,\%$) were purchased from ICON Services. Research grade $N(C_2H_5)_3$ and (*R*)-3-methylcyclohexanone (98%, *ee* = 99%) were supplied by Aldrich.

Synthesis of the substrates: (*R*)-3-Methyl-1-methylenecyclohexane (**1**) was synthesized from (*R*)-3-methylcyclohexanone (98%, *ee* = 99%) by using Corey's procedure[20] for the Wittig reaction. The same starting chiral ketone was treated with CH_3MgBr in dry diethyl ether to give, after hydrolysis, both (1*R*,3*R*)-1,3-dimethylcyclohexanol (**2*E***) and (1*S*,3*R*)-1,3-dimethylcyclohexanol (**2*Z***). Each diastereomer was initially assigned on the basis of the product ratio (*E*/*Z* = 68:32) reported in the literature,[16] and was further confirmed by NMR spectroscopic analysis of the corresponding methyl ethers (see below). $NaNH_2$ and subsequently CH_3I were added to a stirred sample of the latter crude reaction mixture to afford the diastereomers (1*R*,3*R*)-1-methoxy-1,3-dimethylcyclohexane (**3*E***) and (1*S*,3*R*)-1-methoxy-1,3-dimethylcyclohexane (**3*Z***). All the synthesized compounds were purified by preparative gas–liquid chromatography (GLC) on either a 5 m × 4 mm [inside diameter (i.d.)] stainless steel column packed with 10% Carbowax 20M on 80–100 mesh Chromosorb WAW at 110 °C (Chrompack), or on a 3 m × 4 mm (i.d.) stainless steel column packed with 10% OV-17 on 80–100 mesh Chromosorb WAW at 80 °C (Chrompack). The chemical (> 99.9%) and optical (*ee* ca. 99%) purity of **1**, **2*E***, **2*Z***, **3*E***, and **3*Z*** was verified by analytical GLC by using the same chiral columns that were used for the analysis of the γ-irradiated gaseous mixtures (MEGADEX DACTBS-β (30% 2,3-di-*O*-acetyl-6-*O*-*tert*-butyldimethylsilyl-β-cyclodextrin in OV 1701, 25 m long, 0.25 mm i.d., $d_f = 0.25$ μm), $40 < T < 170$ °C, 2 °C min^{-1}; CP-Chirasil-DEX CB, 25 m long, 0.25 mm i.d., $d_f = 0.25$ μm), $40 < T < 180$ °C, 5 °C min^{-1}). A sample of the ethers **3*E*** and **3*Z*** was analyzed by ^{13}C and ^1H NMR spectroscopy.

Procedure: A greaseless vacuum line was used to prepare the gaseous mixtures according to conventional procedures. The starting chiral substrate and the labeled nucleophile (**1** and $CH_3{}^{18}OH$ or $H_2{}^{18}O$; **2*E*** or **2*Z*** and $H_2{}^{18}O$), as well as a thermal radical scavenger (O_2), and a powerful base [$N(C_2H_5)_3$] (proton affinity = 234.7 kcal mol^{-1})[5a] were introduced into carefully outgassed 130 mL Pyrex bulbs, each equipped with a break-seal tip. The bulbs were filled with 750 Torr of CH_4 (**1**/$CH_3{}^{18}OH$ mixtures), CH_3F (**1**/$H_2{}^{18}O$ mixtures), or CH_3Cl (**2*E*** or **2*Z***/$H_2{}^{18}O$ mixture), cooled to liquid-nitrogen temperature, and sealed off. The gaseous mixtures were then submitted to irradiation at a constant temperature (25–120 °C) in a ^{60}Co source (dose: 1×10^4 Gy; dose rate: 5×10^3 Gy h^{-1}, determined with a neopentane dosimeter). Control experiments, carried out at doses ranging from 1×10^3 to 1×10^5 Gy, showed that the relative yields of products are largely independent of the dose. The radiolytic products were analyzed on the above-mentioned chiral columns by GLC using a Chrompack-9002 gas chromatograph equipped with a flame-ionization detector. The products were identified by comparing their retention volumes with those of authentic standard compounds, and were further confirmed by GLC–MS by using a Hewlett-Packard 5890A gas chromatograph in sequence with a HP-5970B mass spectrometer. The yields were determined from the areas of the corresponding eluted peaks by using the internal standard (i.e., benzyl alcohol) method, and individual calibration factors were used to correct the detector response. Blank experiments were carried out in order to ensure that thermal decomposition of the starting substrates and their ethereal products, as well as the thermal racemization of **1**, and the epimerization of **2*E*** and **2*Z*** was not occurring within the temperature range investigated.

The extent of ^{18}O incorporation into the radiolytic products was determined by GLC–MS, whereby the mass analyzer was set on the selected-ion mode (SIM). The ion fragments at $m/z = 127$ (^{16}O-[$M - CH_3$]$^+$) and $m/z = 129$ (^{18}O-[$M - CH_3$]$^+$) were monitored in order to analyze the **3*E*** and **3*Z*** ethers. The corresponding alcohols **2*E*** and **2*Z*** were examined by using the fragments at $m/z = 113$ (^{16}O-[$M - CH_3$]$^+$) and $m/z = 115$ (^{18}O-[$M - CH_3$]$^+$). The ion fragment at $m/z = 110$ ([M]$^+$) was monitored in order to analyze substrate **1** and any possible isomers.

Computational details: Quantum-chemical calculations were performed by using the GAUSSIAN 98 set of programs.[21] The geometry of the investigated species was optimized at the B3LYP/6–31G* level of theory.[13] The structures corresponding to the critical points were submitted to frequency calculations, at the same level of theory, in order to ascertain their real-minimum or transition-structure character on the PES, and to evaluate the corresponding *ZPE*.[22]

Acknowledgements

This work was supported by the Ministero dell'Istruzione, dell'Università e della Ricerca (MIUR) and the Consiglio Nazionale delle Ricerche (CNR). I wish to express my gratitude to Maurizio Speranza for helpful discussions. I would also like to thank Luisa Mannina, Stéphane Viel, and Annalaura Segre for NMR spectroscopic analysis.

[1] Special Thematic Issue on Diastereoselection; *Chem. Rev.* **1999**, *95*, whole issue.
[2] a) C. K. Cheung, L. T. Tseng, M. H. Lin, S. Srivastava, W. J. le Noble, *J. Am. Chem. Soc.* **1986**, *108*, 1598–1605; corrigendum: C. K. Cheung, L. T. Tseng, M. H. Lin, S. Srivastava, W. J. le Noble, *J. Am. Chem. Soc.* **1987**, *109*, 7239; b) S. Srivastava, W. J. le Noble, *J. Am. Chem. Soc.* **1987**, *109*, 5874–5875; c) W. Adcock, J. Cotton, N. A. Trout, *J. Org. Chem.* **1994**, *59*, 1867–1876; d) R. Herrmann, W. Kirmse, *Liebigs Ann. Chem.* **1995**, 699–702; e) W. Adcock, N. J. Head, N. R. Lokan, N. A. Trout, *J. Org. Chem.* **1997**, *62*, 6177–6182.
[3] A. Filippi, N. A. Trout, P. Brunelle, W. Adcock, T. S. Sorensen, M. Speranza, *J. Am. Chem. Soc.* **2001**, *123*, 6396–6403.
[4] a) A. Rauk, T. S. Sorensen, C. Maerker, J. W. de M. Carneiro, S. Sieber, P. von R. Schleyer, *J. Am. Chem. Soc.* **1996**, *118*, 3761–3762; b) A. Rauk, T. S. Sorensen, P. von R. Schleyer, *J. Chem. Soc. Perkin Trans. 2* **2001**, 869–874.
[5] a) http://webbook.nist.gov/chemistry—Proton affinity: CH_4 = 129.9 kcal mol^{-1}; C_2H_4 = 162.6 kcal mol^{-1}; b) Calculated proton affinity of **1** (this work) = 208.9 kcal mol^{-1}.
[6] R. J. Blint, T. B. McMahon, J. L. Beauchamp, *J. Am. Chem. Soc.* **1974**, *96*, 1269–1278.
[7] Proton affinity: CH_3OH = 180.3 kcal mol^{-1} (ref. [5a]).
[8] Estimated according to: T. Su, W. J. Chesnavitch, *J. Chem. Phys.* **1982**, *76*, 5183–5185.
[9] M. Speranza, A. Troiani, *J. Org. Chem.* **1998**, *63*, 1020–1026.
[10] Direct evidence of the inertness of $(CH_3)_2Cl^+$ ions toward water arose from the observation that ethereal products recovered from the CH_3Cl/**2*E*** or **2*Z***/$H_2{}^{18}O$ mixtures contained less than 3% of the ^{18}O label.
[11] $H_2{}^{16}O$ is an ubiquitous impurity present in the gaseous systems, which is either introduced with the bulk component or formed during radiolysis. As pointed out by A. Troiani, F. Gasparrini, F. Grandinetti, M. Speranza, *J. Am. Chem. Soc.* **1997**, *119*, 4525—4534, the average stationary concentration of $H_2{}^{16}O$ in the irradiated systems is estimated to approach that of the added $H_2{}^{18}O$ (ca. 3 Torr).
[12] This assumption appears even more reasonable if one considers that unit efficiency is expected for the deprotonation of oxonium intermediates by a very strong base such as $N(C_2H_5)_3$.
[13] a) A. D. Becke, *J. Chem. Phys.* **1993**, *98*, 1372–1377, 5648–5652; b) C. Lee, W. Yang, R. G. Parr, *Phys. Rev. B* **1988**, *37*, 785–789.
[14] a) E. L. Eliel, T. J. Brett, *J. Am. Chem. Soc.* **1965**, *87*, 5039–5043, and references therein; b) F. R. Jensen, B. H. Beck, *J. Am. Chem. Soc.* **1968**, *90*, 1066–1067.
[15] W. Koch, M. C. Holthausen, *A Chemist's Guide to Density Functional Theory*, 2nd ed., Wiley-VCH, Weinheim, **1999**.

[16] E. C. Ashby, J. T. Laemmle, *Chem. Rev.* **1975**, *75*, 521 – 546.
[17] a) A. S. Cieplack, B. D. Tait, C. R. Johnson, *J. Am. Chem. Soc.* **1989**, *111*, 8447 – 8462; b) J. Hudec, J. Huke, J. W. Liebeschuetz, *J. Chem. Soc. Perkin Trans. 2*, **1998**, 1129 – 1138.
[18] M. Speranza, A. Filippi, G. Renzi, G. Roselli, F. Grandinetti, *Chem. Eur. J.* **2003**, *9*, 2072 – 2078.
[19] The term troposelectivity has been recently coined (A. Filippi, M. Speranza, *J. Am. Chem. Soc.* **2001**, *123*, 6077 – 82). Strictly speaking it stands for the selectivity of a reagent toward the chiral or prochiral face of a substrate on which it has been generated. In light of the present work, troposelective reactions are as common as the occurrence of slowly interconverting FAs in the gas phase.
[20] R. Greenwald, M. Chaykovsky, E. J. Corey, *J. Org. Chem.* **1963**, *28*, 1128 – 1129.
[21] M. J. Frisch, G. W. Trucks, H. B. Schlegel, G. E. Scuseria, M. A. Robb, J. R. Cheeseman, V. G. Zakrzewski, J. A. Montgomery, Jr., R. E. Stratman, J. C. Burant, S. Dapprich, J. M. Millam, A. D. Daniels, K. N. Kudin, M. C. Strain, O. Farkas, J. Tomasi, V. Barone, M. Cossi, R. Cammi, B. Mennucci, C. Pomelli, C. Adamo, S. Clifford, J. Ochterski, G. A. Petersson, P. Y. Ayala, Q. Cui, K. Morokuma, D. K. Malik, A. D. Rabuck, K. Raghavachari, J. B. Foresman, J. Cioslowski, J. V. Ortiz, A. G. Raboul, B. B. Stefaniv, G. Liu, A. Liashenko, P. Piskorz, I. Nanayakkara, C. Gonzales, M. Challacombe, P. M. W. Gill, B. Johnson, W. Chen, M. W. Wong, J. L. Andres, C. Gonzales, M. Head-Gordon, E. S. Replogle, J. A. Pople, GAUSSIAN 98, Revision A7, Gaussian Inc., Pittsburg, PA, **1998**.
[22] A. P. Scott, L. Radom, *J. Phys. Chem.* **1996**, *100*, 16502 – 16513.

Received: February 18, 2003
Revised: May 28, 2003 [F4859]

